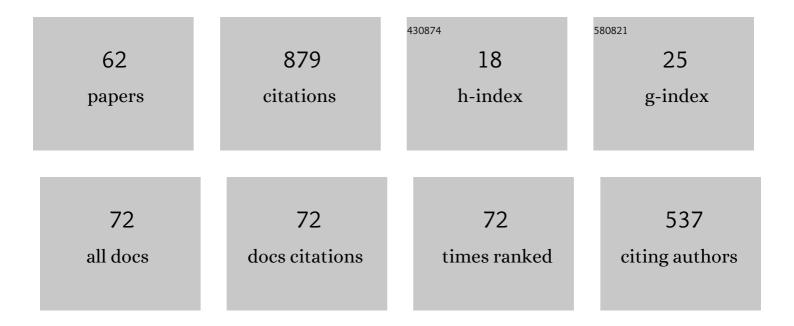
List of Publications by Year in descending order

Source: https://exaly.com/author-pdf/4121545/publications.pdf Version: 2024-02-01



#	Article	IF	CITATIONS
1	Echo occurrence in the southern polar ionosphere for the SuperDARN Dome C East and Dome C North radars. Polar Science, 2021, 28, 100684.	1.2	3
2	E HAIM as a Model of Total Electron Content: Performance and Diagnostics. Space Weather, 2021, 19, e2021SW002872.	3.7	8
3	A Comparison of the Topside Electron Density Measured by the Swarm Satellites and Incoherent Scatter Radars Over Resolute Bay, Canada. Radio Science, 2021, 56, e2021RS007326.	1.6	8
4	Comparison of SuperDARN peak electron density estimates based on elevation angle measurements to ionosonde and incoherent scatter radar measurements. Earth, Planets and Space, 2020, 72, 43.	2.5	6
5	Velocity of SuperDARN Echoes at Intermediate Radar Ranges. Radio Science, 2020, 55, .	1.6	1
6	A Comparison of Crossâ€Track Ion Drift Measured by the Swarm Satellites and Plasma Convection Velocity Measured by SuperDARN. Journal of Geophysical Research: Space Physics, 2019, 124, 4710-4724.	2.4	17
7	Occurrence of F region echoes for the polar cap SuperDARN radars. Earth, Planets and Space, 2019, 71, .	2.5	8
8	Interhemispheric Asymmetry of the Sunward Plasma Flows for Strongly Dominant IMF <i>B</i> <sub><i>Z</i></sub> Â>Â0. Journal of Geophysical Research: Space Physics, 2018, 123, 315-325.	2.4	5
9	Validation of Clyde River SuperDARN radar velocity measurements with the RISR-C incoherent scatter radar. Annales Geophysicae, 2018, 36, 1657-1666.	1.6	1
10	Large‣cale Comparison of Polar Cap Ionospheric Velocities Measured by RISR , RISRâ€N, and SuperDARN. Radio Science, 2018, 53, 624-639.	1.6	6
11	Examining the Potential of the Super Dual Auroral Radar Network for Monitoring the Space Weather Impact of Solar Xâ€Ray Flares. Space Weather, 2018, 16, 1348-1362.	3.7	23
12	Optimal <i>F</i> Region Electron Density for the PolarDARN Radar Echo Detection Near the Resolute Bay Zenith. Radio Science, 2018, 53, 1002-1013.	1.6	3
13	Seasonal effect for polar cap sunward plasma flows at strongly northward IMF <i>B<sub>z</sub></i> . Journal of Geophysical Research: Space Physics, 2017, 122, 2530-2541.	2.4	7
14	Seasonal and solar cycle variations in the ionospheric convection reversal boundary location inferred from monthly SuperDARN data sets. Annales Geophysicae, 2016, 34, 227-239.	1.6	11
15	Calibration and assessment of Swarm ion drift measurements using a comparison with a statistical convection model. Earth, Planets and Space, 2016, 68, .	2.5	10
16	On the consistency of the SuperDARN radar velocity and <b>E</b> × <b>B</b> plasma drift. Radio Science, 2016, 51, 1792-1805.	1.6	7
17	Statistical study of midlatitude <i>E</i> region echoes observed by the Hokkaido SuperDARN HF radar. Journal of Geophysical Research: Space Physics, 2015, 120, 9959-9976.	2.4	7
18	Longâ€ŧerm variations in the intensity of polar cap plasma flows inferred from SuperDARN. Journal of Geophysical Research: Space Physics, 2015, 120, 9722-9737.	2.4	4

#	Article	IF	CITATIONS
19	Variations in the occurrence of SuperDARN F region echoes. Annales Geophysicae, 2014, 32, 147-156.	1.6	12
20	Hokkaido HF radar signatures of periodically reoccurring nighttime mediumâ€scale traveling ionospheric disturbances detected at short ranges. Journal of Geophysical Research: Space Physics, 2014, 119, 1200-1218.	2.4	6
21	Seasonal and diurnal variations of PolarDARN F region echo occurrence in the polar cap and their causes. Journal of Geophysical Research: Space Physics, 2014, 119, 10,426.	2.4	16
22	Electron density and electric field over Resolute Bay andFregion ionospheric echo detection with the Rankin Inlet and Inuvik SuperDARN radars. Radio Science, 2014, 49, 1194-1205.	1.6	10
23	Poker Flat Incoherent Scatter Radar observations of anomalous electron heating in the E region. Annales Geophysicae, 2013, 31, 1163-1176.	1.6	5
24	Signatures of moving polar cap arcs in the F-region PolarDARN echoes. Annales Geophysicae, 2012, 30, 441-455.	1.6	9
25	Response of ionospheric convection to sharp southward IMF turnings inferred from magnetometer and radar data. Journal of Geophysical Research, 2012, 117, .	3.3	12
26	Interplanetary magnetic field control and magnetic conjugacy of auroral <i>E</i> region backscatter. Journal of Geophysical Research, 2012, 117, .	3.3	2
27	Resolute Bay CADI ionosonde drifts, PolarDARN HF velocities, and cross polar cap potential. Radio Science, 2012, 47, .	1.6	9
28	Velocity of E-region HF echoes under strongly-driven electrojet conditions. Annales Geophysicae, 2012, 30, 235-250.	1.6	19
29	Monitoring the F-region peak electron density using HF backscatter interferometry. Geophysical Research Letters, 2011, 38, n/a-n/a.	4.0	21
30	Dependence of spectral width of ionosphericFregion HF echoes on electric field. Journal of Geophysical Research, 2011, 116, n/a-n/a.	3.3	3
31	Volume cross section of auroral radar backscatter and RMS plasma fluctuations inferred from coherent and incoherent scatter data: a response on backscatter volume parameters. Annales Geophysicae, 2011, 29, 1081-1092.	1.6	6
32	Spherical cap harmonic analysis of Super Dual Auroral Radar Network (SuperDARN) observations for generating maps of ionospheric convection. Journal of Geophysical Research, 2010, 115, .	3.3	16
33	HF ground scatter from the polar cap: Ionospheric propagation and ground surface effects. Journal of Geophysical Research, 2010, 115, .	3.3	23
34	Refractive index effects on the scatter volume location and Doppler velocity estimates of ionospheric HF backscatter echoes. Annales Geophysicae, 2009, 27, 4207-4219.	1.6	50
35	On the SuperDARN cross polar cap potential saturation effect. Annales Geophysicae, 2009, 27, 3755-3764.	1.6	11
36	Threeâ€way validation of the Rankin Inlet PolarDARN radar velocity measurements. Radio Science, 2009, 44, .	1.6	16

#	Article	IF	CITATIONS
37	Time evolution of the subauroral electric fields: A case study during a sequence of two substorms. Journal of Geophysical Research, 2009, 114, .	3.3	19
38	Coordinated observations of nighttime mediumâ€scale traveling ionospheric disturbances in 630â€nm airglow and HF radar echoes at midlatitudes. Journal of Geophysical Research, 2009, 114, .	3.3	16
39	<i>PCN</i> magnetic index and average convection velocity in the polar cap inferred from SuperDARN radar measurements. Journal of Geophysical Research, 2009, 114, .	3.3	21
40	Dependence of SuperDARN cross polar cap potential upon the solar wind electric field and magnetopause subsolar distance. Journal of Geophysical Research, 2008, 113, .	3.3	13
41	Aspect angle dependence of the <i>E</i> region irregularity velocity at large flow angles. Journal of Geophysical Research, 2007, 112, .	3.3	13
42	A comparison of CADIâ€inferred <i>F</i> region plasma convection and DMSP ion drift above Resolute Bay. Radio Science, 2007, 42, .	1.6	3
43	Heights of SuperDARN F region echoes estimated from the analysis of HF radio wave propagation. Annales Geophysicae, 2007, 25, 1987-1994.	1.6	11
44	STARE velocity at large flow angles: is it related to the ion acoustic speed?. Annales Geophysicae, 2006, 24, 873-885.	1.6	5
45	Observations of high-velocity SAPS-like flows with the King Salmon SuperDARN radar. Annales Geophysicae, 2006, 24, 1591-1608.	1.6	29
46	A first comparison of irregularity and ion drift velocity measurements in the E-region. Annales Geophysicae, 2006, 24, 2375-2389.	1.6	7
47	A study of aspect angle effects in theE-region irregularity velocity using multi-point electric field measurements. Geophysical Research Letters, 2006, 33, .	4.0	10
48	Comparison of DMSP cross-track ion drifts and SuperDARN line-of-sight velocities. Annales Geophysicae, 2005, 23, 2479-2486.	1.6	48
49	On the relationship between the velocity of E-region HF echoes and <i>E</i> x <i>B</i> plasma drift. Annales Geophysicae, 2005, 23, 371-378.	1.6	30
50	Simultaneous HF measurements of E- and F-region Doppler velocities at large flow angles. Annales Geophysicae, 2004, 22, 1177-1185.	1.6	24
51	Seasonal variation of HF radarFregion echo occurrence in the midnight sector. Journal of Geophysical Research, 2004, 109, .	3.3	29
52	Observations of double-peakedEregion coherent spectra with the CUTLASS Finland HF radar. Radio Science, 2004, 39, n/a-n/a.	1.6	6
53	IMF By effects in the magnetospheric convection on closed magnetic field lines. Geophysical Research Letters, 2003, 30, .	4.0	25
54	Substorm onset times as derived from geomagnetic indices. Geophysical Research Letters, 2002, 29, 134-1-134-4.	4.0	11

#	Article	IF	CITATIONS
55	Multifrequency measurements of HF Doppler velocity in the auroralEregion. Journal of Geophysical Research, 2002, 107, SIA 25-1-SIA 25-12.	3.3	13
56	On the factors controlling occurrence of F-region coherent echoes. Annales Geophysicae, 2002, 20, 1385-1397.	1.6	34
57	Velocities of auroral coherent echoes at 12 and 144 MHz. Annales Geophysicae, 2002, 20, 1647-1661.	1.6	19
58	Observations of 50- and 12-MHz auroral coherent echoes at the Antarctic Syowa station. Journal of Geophysical Research, 2001, 106, 12875-12887.	3.3	20
59	On the power-velocity relationship for 12- and 50-MHz auroral coherent echoes. Journal of Geophysical Research, 2001, 106, 15455-15469.	3.3	12
60	SuperDARN convection and Sondrestrom plasma drift. Annales Geophysicae, 2001, 19, 749-759.	1.6	25
61	CUTLASS HF radar observations of high-velocity E-region echoes. Annales Geophysicae, 2001, 19, 411-424.	1.6	15
62	Evolution of ionospheric multicell convection during northward interplanetary magnetic field with  Bz/By  > 1. Journal of Geophysical Research, 2000, 105, 27095-27107.	3.3	40